A Quantitative Single-Molecule Study of Thioether Molecular Rotors

Ashleigh E. Baber, Heather L. Tierney, and E. Charles H. Sykes*

Department of Chemistry, Tufts University, Medford, Massachusetts 02155-5813

ARTICLE

ABSTRACT This paper describes a fundamental, single-molecule study of the motion of a set of thioethers supported on Au surfaces. Thioethers constitute a simple, robust system with which molecular rotation can be actuated both thermally and mechanically. Low-temperature scanning tunneling microscopy allowed the measurement of the rotation of individual molecules as a function of temperature and the quantification of both the energetic barrier and pre-exponential factor of the motion. The results suggest that movement of the second CH_2 group from the S atom over the surface is responsible for the barrier. Through a series of single-molecule manipulation experiments, we have switched the rotation on and off reversibly by moving the molecules toward or away from one another. Arrhenius plots for individual dibutyl sulfide molecules reveal that the torsional barrier to rotation is ~1.2 kJ/mol, in good agreement with the temperature at which the molecule's appearance changes from a linear to a hexagonal shape in the STM images. The thioether backbone constitutes an excellent test bed for studying the details of molecular rotation at the single-molecule level.

KEYWORDS: molecular rotor · thioether · STM · single-molecule measurement · Au{111} · rotation

Molecular motors are ubiquitous in nature; they perform tasks as varied as organizing the cellular cytoplasm by vesicle transport (*i.e.*, kinesin or dynein) to powering the motion of cells (*i.e.*, the bacterial flagellar motor) and even driving whole body locomotion through muscle contraction.[1] In stark contrast to nature, current manmade devices (with the exception of liquid crystals) make no use of nanoscale molecular motion. This is due in part to a gap in the understanding of how individual molecular components behave in the face of opposing forces such as friction, thermal fluctuations, viscosity, and coupling to neighbors. The majority of current understanding of molecular rotors has been generated by synthesizing complex organic structures and studying their properties in solution.[2−7] Complex functionality has been developed that allows either chemically driven[2] or photon-driven[6] unidirectional motion. Simulations have also revealed many important aspects of the complex workings of both the biological and chemical systems.[8−12]

In nature, motors operate at interfaces, and thus surface-mounted rotors offer the most potential for nanoscience.[13] Therefore, mastering the properties of surface-bound rotors is the next logical step toward harnessing their utility. Studying the rotation of molecules bound to surfaces offers the advantage that a single layer can be assembled and monitored using the tools of surface science. This approach allows for the engineering of artificial molecular machinery that can respond to electrical and optical stimuli and perform useful work such as driving fluid flow. One of the earliest surface studies of thermally induced molecular rotation of PF_3 on Ni{111} was reported by the Yates group in 1987.[14]

The first scanning probe measurements of individual rotational events were made in 1993 when the STM tip was used to induce the rotation of antimony dimers on a Si(001) surface.[15] Gimzewski performed the first study of the rotation of a single molecule. His group found that individual porphyrins in an ordered network could be manipulated into vacancies where they spun very fast at room temperature (>30 kHz) and then reversibly locked back into position in the network.[16,17] Over the last 10 years, several other groups have studied the rotation of porphyrins on surfaces with STM.[18−24] Temperature-dependent imaging has allowed the rotational barrier to be quantified,[19,20] and Lambert and coworkers demonstrated that rotation could be actuated by adsorbing a simple ligand that lifted a static porphyrin off the surface and allowed facile rotation.[21]

Apart from porphyrins, there is only a small amount of data on the rotation of surface-bound molecules. Ho and coworkers studied O_2 molecules on Pt{111}

*Address correspondence to charles.sykes@tufts.edu.

Received for review August 5, 2008 and accepted September 30, 2008.

Published online October 10, 2008.
10.1021/nn800497y CCC: $40.75

© 2008 American Chemical Society

and found that the molecule had three equivalent orientations on the Pt{111} surface.[25] Single electrons with energy >0.175 eV were found to induce rotation of the molecule. The same group also studied acetylene on Cu{100} and found that excitation of the C−H bonds *via* inelastic electron tunneling (IET) increased the rate of rotation.[26] Acetylene was used by the Salmeron and Kawai groups to investigate rotation.[27,28] Kawai also reported the IET induced rotation of *cis*-2-butene motion on Pd{110}.[29,30] The Michl group has made many contributions to the surface-mounted rotor field by combining theory and experiments.[13,31−37] This group measured the dielectric response of monolayer films of chloromethyl- and dichloromethylsilyl dipolar rotors on fused silica as a function of coverage and modeled the barrier heights with molecular mechanics.[36] The group has also synthesized both polar and nonpolar rotors and shown that the electric field produced by an STM tip can be used to produce an orientation change only in the polar rotor.[38]

Other work of particular relevance to this paper includes studies by the Bartels group, who studied halogenated thiophenol molecules on a Cu{111} surface.[39,40] They found that the molecules rotated freely at temperatures as low as 15 K until the S−H bond was cleaved by tunneling electrons and rotation ceased. The Yates group observed similar rotation of CH_3SH on Au{111} and used DFT calculations to explain the low barrier to rotation.[41] In both of these studies, the rotating molecules appeared in the STM images as hexagons due to the preferred orientations of the molecules on the three-fold symmetric Cu and Au surfaces.

This paper describes a simple rotor system of thioether (RSR) molecules of varying length which bind to the Au{111} surface through a S−Au bond (the axle) and the alkyl tails (rotor) interact weakly with the surface. A variety of commercially available thioether molecules allow the length of the thioether, and hence the moment of inertia of the molecular rotor, to be varied in a controlled manner.

RESULTS AND DISCUSSION

Au{111} was chosen as a support for thioethers due to both its inertness and the strength of its bonds to S-containing molecules. Au{111} has a unique structure, most commonly referred to as the herringbone, or more technically, the $22 \times \sqrt{3}$ reconstruction.[42,43] Initial experiments on the rotation of thioether molecules involved depositing the molecules on the cold Au{111} surface, then studying their appearance in the regular STM imaging mode as the sample was slowly heated. Figure 1 shows an STM image of 0.08 ML of dibutyl sulfide deposited at 7.6 K and imaged between 7.6 and 25 K. At 7.6 K, the molecules appeared linear and positioned in three preferred orientations that align with the close-packed directions of the Au{111} substrate. Scanning for several minutes at 7.6 K yielded no change

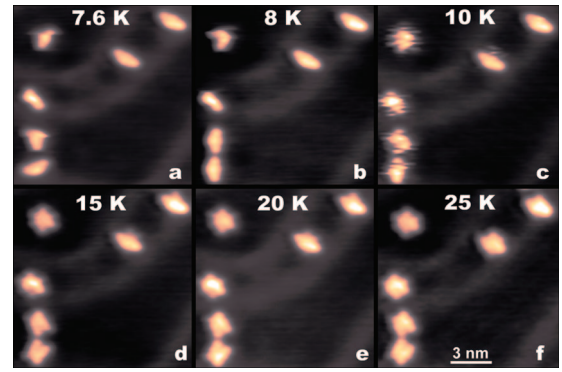

Figure 1. STM images showing thermally induced rotation of dibutyl sulfide; $V_{tip} = -0.3$ V, $I = 10$ pA. At temperatures below 10 K (panels a,b), dibutyl sulfide appears linear in shape and fixed in position on the surface. Above 15 K (panels e,f), the molecules rotate faster than the imaging rate and appear hexagonal in shape.

in appearance or motion of the molecules; therefore, the conditions used for imaging ($V_{tip} = -0.3$ V, $I = 10$ pA) did not perturb the molecules. The sample was then slowly warmed at ~1 K/min and continuously imaged. By constantly correcting for thermal drift, the same set of molecules could be tracked over a temperature range of ~50 K. Figure 1 reveals that at a temperature of ~10 K the images of the molecules became streaky, and at a temperature of 25 K, the molecules no longer looked linear but appeared hexagonal in shape. It is important to note that the molecules all remained in exactly the same area of the surface and hence the same adsorption sites during the warming experiments. Restricting the translational motion of the molecules *via* a strong S−Au bond meant that the only type of motion detectable *via* STM was rotation. This rotational motion of dibutyl sulfide should be reasonably facile, as the alkyl tails are only weakly interacting with the Au surface. Therefore, we attributed the molecules' change in shape as being due to the onset of rotation of the molecules about the central S−Au axle as the temperature was increased. Two other groups have reported similar STM images of rotating molecules. Bartels and co-workers studied a set of benzene thiols on Cu{111} and found that their hexagonal appearance in STM images resulted from registry of the molecule in the six equivalent directions of the Cu{111} surface.[39,40] Voltage pulses from the STM tip allowed the S−H bond to be cleaved, and the covalent S−Cu bond formed tethered the molecule in place and halted the rotation.[40] Yates and co-workers performed a study of methanethiol on Au{111} and found that even at 5 K the intact molecule rotates and appears as a hexagonal shape in STM images.[41,44]

STM movies of dibutyl sulfide at 78 K revealed that even at this elevated temperature (~60 K above the onset of rotation), the molecules diffuse across the surface very slowly (~0.1 Hz) compared to the rate at which they spin ($\sim 1 \times 10^7$ Hz at 78 K). This diffusion rate was calculated by counting the hopping rate of

molecules in time-lapse STM imaging experiments. The rotational rate at 78 K is too fast to be measured by STM; therefore, the rotation rate at 78 K was calculated by extrapolating the Arrhenius plot in Figure 5.

The fact that the molecules rotate quickly and translate slowly makes them an ideal test bed for the study of surface-bound molecular rotation. Another piece of evidence that supports the interpretation that the hexagonal appearance of the molecules is due to rotation is that, upon cooling, the molecules return to imaging as linear shapes. Care was taken during the heating experiments to image with gap conditions that did not perturb or rotate the molecules. It was found that while using voltages between 0.2 and 0.35 V and tunneling currents less than 50 pA the molecules could be imaged for many hours without perturbation of their shape or position. Measuring molecular rotation using nonperturbative conditions is crucial in terms of quantifying the thermally induced motion of molecules without error due to tip-induced rotational effects.

A discussion of any type of rotational motion typically begins with the rigid rotor model.[45] This simple model assumes that the rotor is composed of two point masses connected by a rigid rod. Macroscopically, one would expect that the longer the rotor (and the larger its moment of inertia) the more thermal energy it would require to begin rotating. Quantum mechanically, however, the solution to the rigid rotor problem reveals that increasing the moment of inertia will decrease the energetic gap between ground and first rotationally excited state, and hence longer, heavier rotors should have their excited rotational levels populated at lower temperatures than shorter, lighter rotors. The rigid rotor model works well for quantifying gas phase molecular rotation; *however*, as it assumes a flat torsional potential, it is not necessarily accurate for describing surface-mounted rotors, for which the interaction with the surface imposes a nonzero torsional potential.[13] These systems are much better described in terms of the height of the torsional barrier which dictates the onset of thermally induced rotational motion.

In order to investigate the effect of the rotor's size (or more technically its moment of inertia) on its rotational barrier, a series of thioethers from dimethyl to dihexyl sulfide were studied as a function of temperature. When studying thioethers with different tail lengths, just as with dibutyl sulfide, scanning conditions were used that did not cause tip-induced rotation. Figure 2 reveals the effect of temperature on this set of molecules. At 7.6 K, all of the molecules, with the exception of dimethyl sulfide, imaged as linear shapes, which corresponds to the molecules being static on the surface. Dimethyl sulfide imaged as a hexagon (rotating) under all scanning conditions ($0.05 \leq V_{tip} \leq 1$ V/$2 \leq I \leq 1000$ pA) and all temperatures studied (7.6−78 K). Interestingly, diethyl, dibutyl, and dihexyl sulfide all began to rotate fully at 16 ± 2 K.

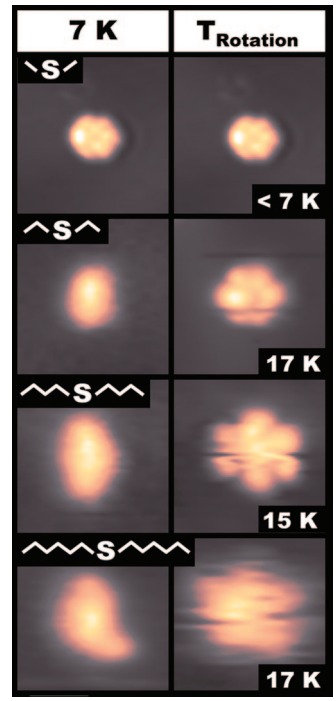

Figure 2. STM images showing thermal activation of thioether rotors: dimethyl, diethyl, dibutyl, and dihexyl sulfide. Temperatures in the right column indicate the onset of rotation. Scale bar = 1 nm. $V_{tip} = -0.3$ V, $I = 9$ pA.

This result reveals that dimethyl sulfide has a very low barrier to rotation, whereas all the other molecules have roughly the same energetic barrier to rotation. As expected, neither the classical nor quantum mechanical picture for the rigid rotor accurately describes the behavior of the thioether rotor system. Clearly, the interaction of diethyl, dibutyl, and dihexyl sulfide with the surface imposes a torsional potential that governs the rotational motion of the molecules. These results can be understood by considering the conformation of the molecule relative to the surface. Dimethyl sulfide has just two methyl groups that point up off the surface, whereas diethyl, dibutyl, and dihexyl sulfide have two or more carbons in the alkyl tail in which the second carbon atom points down at the surfaces (Scheme 1). The fact that the jump in energetic barrier occurs after adding a second carbon to the chain suggests that the barrier to rotation originates from the motion of this CH_2 group over the surface (Scheme 1). Dimethyl sulfide's geometry renders it with a very low barrier (<0.5 kJ/mol) and almost unhindered rotational motion.

The fact that all the molecules larger than dimethyl sulfide begin to rotate at the same temperature suggests that the most significant contribution to the ener-

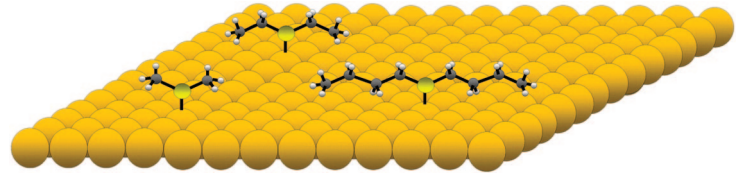

Scheme 1. Dimethyl, Ethyl, and Butyl Sulfide on Au{111}

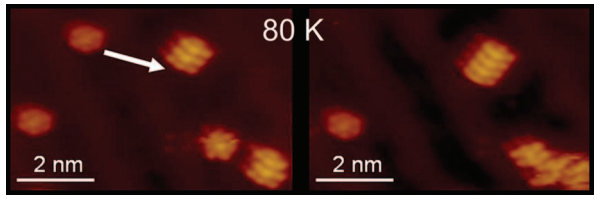

Figure 3. Rotation can be mechanically controlled by the proximity of surrounding molecules. STM images showing how the rotation of an individual dibutyl sulfide molecule can be switched off by maneuvering it toward a static chain of three molecules; $V_{tip} = -0.3$ V, $I = 15$ pA, temp = 78 K.

getic barrier comes from the interaction of the second carbon of the alkyl chain with the surface and that adding additional CH_2 groups to the alkyl tail does not affect the torsional barrier significantly. We hypothesize that the torsional barrier of diethyl, dibutyl, and dihexyl sulfide derives from interaction of the second CH_2 group from the S−Au axle and that modification of this position may provide a method to controllably adjust the torsional potential of thioether rotors.

It is also interesting to note that the shorter molecules (dibutyl sulfide and smaller) image as hexagonal shapes when rotating, whereas images of rotating dihexyl sulfide were less defined even with sharp STM tips and the molecules appeared as roughly circular shapes. The "sharpness" of an STM tip refers to the resolution with which it can image a nanometer-scale feature such as a molecule. Sharper tips reveal more internal resolution of surface features and molecular adsorbates. The fact that even sharp tips never image dihexyl sulfide clearly (Figure 2) is most probably due to the longer alkyl tails of dihexyl sulfide having more degrees of freedom and being less rigidly locked to the surface in three equivalent orientations as the shorter thioethers are.

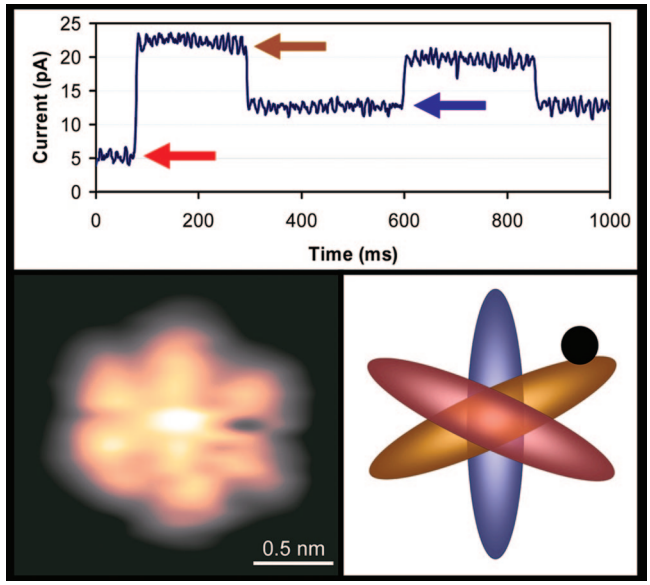

Figure 4. Tunneling current as a function of time (*I vs t*) plots indicate changes in the position of the alkyl tail of the thioether with respect to the STM tip and hence the rotation rate of the molecule. The *I vs t* curves reveal three levels of tunneling current that correspond to the three inequivalent orientations of dibutyl sulfide (blue, yellow, and red) with respect to the STM tip position (black dot). STM images like that shown allowed the tip to be placed asymmetrically over the molecule for *I vs t* measurements.

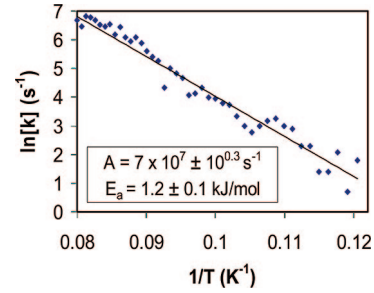

Figure 5. Arrhenius plot for the rotation of an individual dibutyl sulfide molecule in an fcc area on the Au{111} surface. Rates are obtained from switching events in *I vs t* curves at each temperature under nonperturbative tunneling conditions.

In order to test the possibility of actuating molecular rotation mechanically, molecular manipulation experiments were performed. Figure 3 shows an STM image of dibutyl sulfide molecules at 78 K. The arrow in the upper left image shows how the STM tip can be maneuvered to shift one rotating molecule toward a group of three static molecules that are locked together by van der Waals interactions between the alkyl tails.[46] The molecular manipulation was achieved by moving the tip over the rotating molecule, reducing the tunneling voltage to 0.05 V and increasing the current to 120 nA, moving the tip to the desired location, and then returning the gap to normal scanning conditions. The feedback loop remained on during the whole manipulation procedure. Inspection of the right image in Figure 3 reveals that the dibutyl sulfide molecule has stopped spinning and joined the chain. This is because as the molecules were brought together they were attracted by van der Waals forces between the alkyl tails, and this interaction hinders each other's rotation.[46,47] Our data revealed that this process was reversible; if a molecule was pulled off a static chain at 78 K, it began to rotate again. Using similar procedures, straight rigid chains of >10 molecules were built and then disassembled back into rotating monomers at 78 K.

In order to measure the rate at which dibutyl sulfide rotated as a function of temperature, tunneling current *versus* time (*I vs t*) experiments were performed. As the molecule rotated, the alkyl tails passed under the STM tip causing the tunneling current to fluctuate. If the tip was placed asymmetrically to the side of one of the six lobes of the molecule, the tunneling current alternated between three discrete values (see Figure 4). These three values corresponded to the three inequivalent orientations of the molecule with respect to the STM tip. This point refers to the position of the tip with respect to the molecule as it rotates beneath it. At rest, the molecule images as a linear shape, whereas the spinning molecule images as a hexagon; therefore, the molecule resides more often in three orientations on

the surface. In order to distinguish between the three orientations using *I vs t* spectroscopy, the tip was placed slightly to the side of one of the three positions. This break in symmetry yielded three distinct levels of tunneling current (as shown in Figure 4) that correlate with the three inequivalent orientations of the molecule with respect to the tip. The highest tunneling current corresponded to the orientation of the molecule (shaded in yellow) almost directly under the tip (black dot). The next highest tunneling current corresponded to the molecule lying in the orientation shaded in blue, and the lowest current reading came from the molecule lying at an angle that left it furthest from the tip (shaded in red). These three-state *I vs t* plots allowed the direction of rotation of individual molecules to be monitored over many hundreds of rotations. As would be expected from the second law of thermodynamics, it was found that thermal excitation gave a random progression of rotational direction.[10−12] The molecule essentially flipped randomly between states with no knowledge of the previous state.

Performing *I vs t* experiments while heating the sample allowed for the measurement of the rate of rotation of individual molecules as a function of temperature. Care was taken to record these data under tunneling conditions that did not excite the molecule. An Arrhenius plot for dibutyl sulfide in an fcc region on Au{111} is shown in Figure 5. These measurements yielded an activation barrier (E) of 1.2 ± 0.1 kJ/mol and an attempt frequency (A) of $7 \times 10^{7\pm0.3}$ Hz for molecules in the fcc areas of the Au{111} surface. A comparison of the rates measured by *I vs t* curves and the temperature-dependent imaging experiments shown in Figure 1 reveals that the two methods for measuring the thermal activation of molecular rotation are comparable, and the results do not contradict each other. In regular STM imaging mode, the molecules appear as hexagons when they start to rotate faster than the imaging rate. The data in Figure 1 were recorded at a scan rate of ~10 lines/s. This meant that a molecule rotating at a rate >1000 Hz appeared to be in all three equivalent positions on the time scale of scanning and imaged with a hexagonal shape. Placing this rate in the Arrhenius equation along with the molecule's activation energy and attempt frequency derived from the Arrhenius plots gave a rotational onset temperature for dibutyl sulfide of 13 ± 2 K, in good agreement with the value (15 ± 2 K) measured by regular STM imaging as a function of temperature in Figure 1. This comparison of methods for measuring a molecule's rate of rotation as a function of temperature demonstrates that, while the Arrhenius approach is more accurate, both temperature-dependent imaging and Arrhenius measurements essentially monitor the same phenomena, namely, the onset of molecular rotation as a function of temperature.

Attempt frequencies that differ from the normal range ($10^{10}-10^{13}$ Hz) often give clues to the mechanism by which the motion occurs. Assuming a potential that is proportional to the square of the rotational angle and has a maximum value of 1.2 kJ/mol at ±30° from the minima, classically one would expect an attempt frequency around 10^{11} Hz for the present system. The low attempt frequency ($7 \times 10^{7\pm0.3}$ Hz) measured experimentally for dibutyl sulfide hints at a multistep process leading to molecular rotation. The fact that the molecule is symmetric means that both rotor arms must overcome the torsional barrier simultaneously and in phase with one another. We hypothesize that this constraint is responsible for the low A value measured experimentally and are currently performing experiments with asymmetric thioether rotors to further investigate this phenomenon.

CONCLUSIONS

Monitoring the thermally induced rotation of a set of symmetric thioethers with variable temperature STM revealed that the second CH_2 group from the S atom is responsible for the barrier to rotation in molecules larger than dimethyl sulfide. Through a series of controlled manipulation experiments, the rotation could be switched on and off reversibly by moving the molecules toward or away from one another. When two dibutyl sulfide molecules are in close proximity, their rotation becomes hindered due to van der Waals interactions between the alkyl tails. Tunneling current *versus* time spectra taken at specific locations on the molecules revealed three distinct states from which the orientation of the molecule and the direction of its rotation could be measured. Arrhenius plots for individual molecules revealed that the barrier to rotation was 1.2 ± 0.1 kJ/mol, in good agreement with the temperature at which the onset of rotation was observed in the regular STM imaging mode. The thioether backbone serves as an excellent test bed for studying the fundamentals of surface-bound molecular rotation. Future work will involve the study of dipolar rotors, asymmetric rotors, molecules functionalized with groups that impart an asymmetric torsional potential, and rotational coupling between adjacent molecules.

MATERIALS AND METHODS

All STM experiments were performed in a low-temperature, ultrahigh vacuum (LT-UHV) microscope built by Omicron.[48] The Au{111} sample purchased from MaTecK was prepared by cycles of Ar^+ sputtering (1.5 keV/10 μA) for 30 min followed by a 2 min anneal to 1000 K. Approximately 12 of these sputter/anneal cycles were performed upon receiving the crystal, followed by a further 2 sputter/anneal cycles between each STM experiment. After the final anneal, the crystal was transferred in less than 5 min in vacuum ($<5 \times 10^{-10}$ mbar) to the precooled STM

chamber. In approximately 30 min, the sample cooled from room temperature to either 78 or 7 K. All images were recorded with etched W tips, and voltages refer to the sample bias. Thioethers (between 99.9 and 99.95% purity) were obtained from Sigma Aldrich and were further purified by cycles of freeze/pump/thaw prior to introduction to the STM chamber *via* a leak valve. The molecules were deposited on the sample by a collimated molecular doser while the tip was scanning. All coverages are quoted in monolayers (ML), where 1 ML refers to a complete, single-layer coverage of the molecule. The STM stage was equipped with a sample heater capable of controllably heating the sample and tip up to 50 K above the base temperature.

Acknowledgment. The authors thank the ACS Petroleum Research Fund, Research Corporation, NSF (Grant #0717978), and the Beckman Foundation for support of this research. A.E.B. thanks the DOEd for a GAANN fellowship.

REFERENCES AND NOTES

1. Schliwa, M.; Woehlke, G. Molecular Motors. *Nature* **2003**, *422*, 759–765.
2. Kelly, T. R.; De Silva, H.; Silva, R. A. Unidirectional Rotary Motion in a Molecular System. *Nature* **1999**, *401*, 150–152.
3. Kelly, T. R.; Silva, R. A.; De Silva, H.; Jasmin, S.; Zhao, Y. J. A Rationally Designed Prototype of a Molecular Motor. *J. Am. Chem. Soc.* **2000**, *122*, 6935–6949.
4. Leigh, D. A.; Wong, J. K. Y.; Dehez, F.; Zerbetto, F. Unidirectional Rotation in a Mechanically Interlocked Molecular Rotor. *Nature* **2003**, *424*, 174–179.
5. Hernandez, J. V.; Kay, E. R.; Leigh, D. A. A Reversible Synthetic Rotary Molecular Motor. *Science* **2004**, *306*, 1532–1537.
6. Koumura, N.; Zijlstra, R. W. J.; van Delden, R. A.; Harada, N.; Feringa, B. L. Light-Driven Monodirectional Molecular Rotor. *Nature* **1999**, *401*, 152–155.
7. van Delden, R. A.; ter Wiel, M. K. J.; Pollard, M. M.; Vicario, J.; Koumura, N.; Feringa, B. L. Unidirectional Molecular Motor on a Gold Surface. *Nature* **2005**, *437*, 1337–1340.
8. Astumian, R. D. Design Principles for Brownian Molecular Machines: How to Swim in Molasses and Walk in a Hurricane. *Phys. Chem. Chem. Phys.* **2007**, *9*, 5067–5083.
9. Astumian, R. D.; Derenyi, I. Fluctuation Driven Transport and Models of Molecular Motors and Pumps. *Eur. Biophys. J.* **1998**, *27*, 474–489.
10. Astumian, R. D. Thermodynamics and Kinetics of a Brownian Motor. *Science* **1997**, *276*, 917–922.
11. Astumian, R. D.; Bier, M. Fluctuation Driven Ratchets—Molecular Motors. *Phys. Rev. Lett.* **1994**, *72*, 1766–1769.
12. Derenyi, I.; Astumian, R. D. Intrawell Relaxation Time: The Limit of the Adiabatic Approximation. *Phys. Rev. Lett.* **1999**, *82*, 2623–2627.
13. Kottas, G. S.; Clarke, L. I.; Horinek, D.; Michl, J. Artificial Molecular Rotors. *Chem. Rev.* **2005**, *105*, 1281–1376.
14. Alvey, M. D.; Yates, J. T.; Uram, K. J. The Direct Observation of Hindered Rotation of a Chemisorbed Molecule—PF3 on Ni(111). *J. Chem. Phys.* **1987**, *87*, 7221–7228.
15. Mo, Y. W. Reversible Rotation of Antimony Dimers on the Silicon (001) Surface with a Scanning Tunneling Microscope. *Science* **1993**, *261*, 886–888.
16. Gimzewski, J. K.; Joachim, C.; Schlittler, R. R.; Langlais, V.; Tang, H.; Johannsen, I. Rotation of a Single Molecule within a Supramolecular Bearing. *Science* **1998**, *281*, 531–533.
17. Joachim, C.; Gimzewski, J. K. In *Single Molecular Rotor at the Nanoscale. Molecular Machines and Motors*; Sauvage, J.-P., Eds.; Springer-Verlag: Berlin, 2001; pp 1−18.
18. Stohr, M.; Wagner, T.; Gabriel, M.; Weyers, B.; Moller, R. Direct Observation of Hindered Eccentric Rotation of an Individual Molecule: Cu-Phthalocyanine on C-60. *Phys. Rev. B* **2002**, *65*, 33404.
19. Wahl, M.; Stohr, M.; Spillmann, H.; Jung, T. A.; Gade, L. H. Rotation−Libration in a Hierarchic Supramolecular Rotor−Stator System: Arrhenius Activation and Retardation by Local Interaction. *Chem. Commun.* **2007**, 1349–1351.
20. Wintjes, N.; Bonifazi, D.; Cheng, F. Y.; Kiebele, A.; Stohr, M.; Jung, T.; Spillmann, H.; Diederich, F. A Supramolecular Multiposition Rotary Device. *Angew. Chem., Int. Ed.* **2007**, *46*, 4089–4092.
21. Vaughan, O. P. H.; Williams, F. J.; Bampos, N.; Lambert, R. M. A Chemically Switchable Molecular Pinwheel. *Angew. Chem., Int. Ed.* **2006**, *45*, 3779–3781.
22. Ye, T.; Takami, T.; Wang, R. M.; Jiang, J. Z.; Weiss, P. S. Tuning Interactions between Ligands in Self-Assembled Double-Decker Phthalocyanine Arrays. *J. Am. Chem. Soc.* **2006**, *128*, 10984–10985.
23. Takami, T.; Ye, T.; Arnold, D. P.; Sugiura, K.; Wang, R. M.; Jiang, J. Z.; Weiss, P. S. Controlled Adsorption Orientation for Double-Decker Complexes. *J. Phys. Chem. C* **2007**, *111*, 2077–2080.
24. Hersam, M. C.; Guisinger, N. P.; Lyding, J. W. Isolating, Imaging, and Electrically Characterizing Individual Organic Molecules on the Si(100) Surface with the Scanning Tunneling Microscope. *J. Vac. Sci. Technol. A* **2000**, *18*, 1349–1353.
25. Stipe, B. C.; Rezaei, M. A.; Ho, W. Inducing and Viewing the Rotational Motion of a Single Molecule. *Science* **1998**, *279*, 1907–1909.
26. Stipe, B. C.; Rezaei, M. A.; Ho, W. Coupling of Vibrational Excitation to the Rotational Motion of a Single Adsorbed Molecule. *Phys. Rev. Lett.* **1998**, *81*, 1263–1266.
27. Dunphy, J. C.; Rose, M.; Behler, S.; Ogletree, D. F.; Salmeron, M.; Sautet, P. Acetylene Structure and Dynamics on Pd(111). *Phys. Rev. B* **1998**, *57*, R12705–R12708.
28. Matsumoto, C.; Kim, Y.; Okawa, T.; Sainoo, Y.; Kawai, M. Low-Temperature STM Investigation of Acetylene on Pd(111). *Surf. Sci.* **2005**, *587*, 19–24.
29. Sainoo, Y.; Kim, Y.; Okawa, T.; Komeda, T.; Shigekawa, H.; Kawai, M. Excitation of Molecular Vibrational Modes with Inelastic Scanning Tunneling Microscopy Processes: Examination through Action Spectra of *cis*-2-Butene on Pd(110). *Phys. Rev. Lett.* **2005**, *95*, 246102.
30. Sainoo, Y.; Kim, Y.; Komeda, T.; Kawai, M.; Shigekawa, H. Observation of *cis*-2-Butene Molecule on Pd(110) by Cryogenic STM: Site Determination Using Tunneling-Current-Induced Rotation. *Surf. Sci.* **2003**, *536*, L403–L407.
31. Vacek, J.; Michl, J. Artificial Surface-Mounted Molecular Rotors: Molecular Dynamics Simulations. *Adv. Funct. Mater.* **2007**, *17*, 730–739.
32. Vacek, J.; Michl, J. Molecular Dynamics of a Grid-Mounted Molecular Dipolar Rotor in a Rotating Electric Field. *Proc. Natl. Acad. Sci. U.S.A.* **2001**, *98*, 5481–5486.
33. Horinek, D.; Michl, J. Molecular Dynamics Simulation of an Electric Field Driven Dipolar Molecular Rotor Attached to a Quartz Glass Surface. *J. Am. Chem. Soc.* **2003**, *125*, 11900–11910.
34. Horinek, D.; Michl, J. Surface-Mounted Altitudinal Molecular Rotors in Alternating Electric Field: Single-Molecule Parametric Oscillator Molecular Dynamics. *Proc. Natl. Acad. Sci. U.S.A.* **2005**, *102*, 14175–14180.
35. Magnera, T. F.; Michl, J. Altitudinal Surface-Mounted Molecular Rotors. *Mol. Mach.* **2005**, *262*, 63–97.
36. Clarke, L. I.; Horinek, D.; Kottas, G. S.; Varaksa, N.; Magnera, T. F.; Hinderer, T. P.; Horansky, R. D.; Michl, J.; Price, J. C. The Dielectric Response of Chloromethylsilyl and Dichloromethylsilyl Dipolar Rotors on Fused Silica Surfaces. *Nanotechnol.* **2002**, *13*, 533–540.
37. Wang, B.; Zheng, X. L.; Michl, J.; Foley, E. T.; Hersam, M. C.; Bilic, A.; Crossley, M. J.; Reimers, J. R.; Hush, N. S. An Azanorbornadiene Anchor for Molecular-Level Construction on Si(100). *Nanotechnol.* **2004**, *15*, 324–332.
38. Zheng, X. L.; Mulcahy, M. E.; Horinek, D.; Galeotti, F.; Magnera, T. F.; Michl, J. Dipolar and Nonpolar Altitudinal Molecular Rotors Mounted on an Au(111) Surface. *J. Am. Chem. Soc.* **2004**, *126*, 4540–4542.

39. Rao, B. V.; Kwon, K. Y.; Liu, A. W.; Bartels, L. 2,5-Dichlorothiophenol on Cu-(111): Initial Adsorption Site and Scanning Tunnel Microscope-Based Abstraction of Hydrogen at High Intramolecular Selectivity. *J. Chem. Phys.* **2003**, *119*, 10879–10884.
40. Rao, B. V.; Kwon, K. Y.; Liu, A. W.; Bartels, L. Measurement of a Linear Free Energy Relationship one Molecule at a Time. *Proc. Natl. Acad. Sci. U.S.A.* **2004**, *101*, 17920–17923.
41. Maksymovych, P.; Sorescu, D. C.; Dougherty, D.; Yates, J. T. Surface Bonding and Dynamical Behavior of the CH_3SH Molecule on Au(111). *J. Phys. Chem. B* **2005**, *109*, 22463–22468.
42. Woll, C.; Chiang, S.; Wilson, R. J.; Lippel, P. H. Determination of Atom Positions at Stacking-Fault Dislocations on Au(111) by Scanning Tunneling Microscopy. *Phys. Rev. B* **1989**, *39*, 7988–7991.
43. Barth, J. V.; Brune, H.; Ertl, G.; Behm, R. J. Scanning Tunneling Microscopy Observations on the Reconstructed Au(111) Surface—Atomic-Structure, Long-Range Superstructure, Rotational Domains, and Surface-Defects. *Phys. Rev. B* **1990**, *42*, 9307–9318.
44. Maksymovych, P.; Sorescu, D. C.; Yates, J. T. Methanethiolate Adsorption Site on Au(111): A Combined STM/DFT Study at the Single-Molecule Level. *J. Phys. Chem. B* **2006**, *110*, 21161–21167.
45. McQuarrie, D. A. *Quantum Chemistry*; University Science Books: Mill Valley, CA, 1983; pp 195−254.
46. Jensen, S. C.; Baber, A. E.; Tierney, H. L.; Sykes, E. C. H. Adsorption, Interaction and Manipulation of Dibutyl Sulfide on Cu{111}. *ACS Nano* **2007**, *1*, 22–29.
47. Jensen, S. C.; Baber, A. E.; Tierney, H. L.; Sykes, E. C. H. Dimethyl Sulfide on Cu{111}: Molecular Self-Assembly and Submolecular Resolution Imaging. *ACS Nano* **2007**, *1*, 423–428.
48. Becker, T.; Hövel, H.; Tschudy, M.; Reihl, B. Applications with a New Low-Temperature UHV STM at 5 K. *Appl. Phys. A: Mater. Sci. Process.* **1998**, *66*, S27–S30.